Thermo-Elastoplastic Study of the Colorado Shale Behaviour

Morteza Mohamadi & Richard Wan
Department of Civil Engineering– University of Calgary, Calgary, Alberta, Canada.

GEOQuébec 2015
Challenges from North to South
Des défis du Nord au Sud

ABSTRACT
The thermo-hydro-mechanical behaviour of shale has gained increasing attention in cap rock integrity assessment of fairly shallow steam injection oil recovery projects in western Canada. The paper presents an integrated experimental/constitutive study of the Colorado shale which serves as a cap rock to underlying oil-rich formations in the Cold Lake area, east-central Alberta, Canada. Results of drained thermal consolidation and isothermal triaxial compression tests at different temperatures on Colorado shale show that: 1) volume changes due to drained heating are greatly influenced by consolidation history, 2) initial elastic moduli of the tested samples decrease with elevation of temperature, and 3) the peak and post-peak failure envelopes are nonlinear and show reduced shear strength at elevated temperatures. These phenomenological mechanisms were implemented in an elastoplastic constitutive model which was used to describe the experimental data. Comparison of the experimental measurements and model calculations verify the usefulness of the model.

RÉSUMÉ
Le comportement thermo-hydro-mécanique des schistes argileux est d'un intérêt capital dans l'évaluation de la stabilité de la couverture de roche au-dessus des réservoirs peu profonds de l'Ouest canadien, durant la récupération du pétrole par injection de vapeur. De ce fait, cet article présente une étude expérimentale et constitutive du schiste argileux du Colorado qui sert de couverture de roche à des formations sous-jacentes, riches en pétrole, dans la région de Cold Lake, au Centre-Est de l'Alberta, Canada. Les résultats de consolidation thermique drainée, et des essais de compression triaxiaux isothermes à différentes températures sur les schistes de Colorado montrent que: 1) les déformations volumétriques en condition drainée dépendent de l'histoire de consolidation, 2) le module initial d'élasticité diminue avec l'élévation de la température, et 3) les surfaces de rupture par cisaillement en pic et post-pic sont non linéaires avec une baisse de résistance pour des températures élevées. Ces mécanismes ont été mis en œuvre dans un modèle phénoménologique pour décrire le comportement élasto-plastique du schiste à partir des données expérimentales. La comparaison des mesures expérimentales et des calculs par modélisation démontre l'utilité du modèle constitutif proposé.

1 INTRODUCTION

The thermo-hydro-mechanical behaviour of shales is of particular interest in Western Canada, due to, among others, the crucial role of the shale caprocks in the steam injection oil recovery projects. Generally speaking, injection of high-pressure steam in a fairly shallow reservoir exposes the overlying shale caprock to highly anisotropic thermo-mechanical stresses which may lead to material failure with many adverse environmental impacts (Carlson 2012; Collins 2007). This has led to a growing recognition of the need for a robust constitutive model that is capable of accurately describing the non-isothermal behaviour of shales.

The thermo-hydro-mechanical behaviour of deep natural clays/shales has been extensively studied in the past with regard to nuclear waste disposal, e.g. Boom clay (Baldi et al. 1988; Sultan et al. 2002), Pasquasia clay (Hueckel and Baldi 1990), Pondita clay (Baldi et al. 1988) and Opalinusclaystone(Monfared et al. 2011). In view of these studies as well as those performed on reconstituted clayey soils, e.g. (Cekerevac and Laloui 2004; Tanaka et al. 1997; Towhata et al. 1993), three major phenomenological elastoplastic mechanisms can be identified, i.e. the temperature-dependence of elastic parameters, yield locus and the plastic strain rate.

In order to describe these mechanisms, several non-isothermal constitutive models with different underlying assumptions have been proposed, e.g. (Abuel-Naga et al. 2009; Cui et al. 2000; Graham et al. 2001; Hamidi et al. 2015; Hueckel and Borsetto 1990; Laloui and Cekerevac 2003; Liu and Xing 2009; Robinet et al. 1996; Yao and Zhou 2013; Zhang et al. 2012; Zhou and Ng 2015). Although these constitutive models can capture certain aspects of the thermo-mechanical behaviour of clays/shales, none of them can describe the simultaneous effects of the temperature variations and destructuration. The latter refers to degradation of an enhanced interparticle bonding which had developed during sedimentation and post-sedimentation history of natural clays/shalesas a result of digenesis (Burland 1990; Leroueil and Vaughan 1990). It was only recently that Nakai et al. (2011) proposed a thermomechanical model to describe the temperature-dependent behaviour of the structured clays. They introduced a new temperature-dependent state variable to describe the parallel downward shift of the normal consolidation line at elevated temperatures. However, their model is limited in the sense that it does not account for temperature-dependence of the elastic parameters, nor does it consider the thermal variability of the critical friction angle.

Based on the lab experimental observations, this paper aims to reformulate and extend the constitutive model of Nakai et al. (2011) to describe the effects of temperature on the mechanical behaviour of the Colorado shale. The generic formulation of the loading yield curves with coupled thermoelastic strains are derived and utilized to extend the subloading and normal-yield surface to non-isothermal conditions. It is shown that the model reduces to that described in Nakai et al. (2011) by choosing specific material parameters. The adequacy of the proposed model is verified using the lab experimental results on the Colorado shale.

2 SUMMARY OF EXPERIMENTAL OBSERVATIONS ON THE COLORADO SHALE

Colorado shale is a dark brown marine shale serving as a cap rock to underlying oil-rich formations in Cold Lake area, east-central Alberta, Canada. Given its important role as a hydraulic seal to the injected fluid in Steam Assisted Gravity Drainage (SAGD) projects, Colorado shale was comprehensively studied in a series of isothermal triaxial compression test at different temperatures as well as p(mean effective stress)-constant tests in the Rock Mechanics Laboratory at the University of Calgary. Authors have presented the elaborate discussion of the corresponding experimental results in (Mohamadi and Wan 2015b) to which the interested reader is referred. The most important observations relevant to the present study are summarized as follows:

1. All samples in triaxial compression tests initially densified and strain hardened until reaching the peak deviatoric stress and strain softened thereafter to reach a nearly constant post-peak deviatoric stress.Strain softening was accompanied with formation of a clearly defined shear plane occurring at an axial strain of 0.55 to 1%.
2. The initial stiffness determined from triaxial compression tests decreased at elevated temperatures quite pronouncedly between 25 and 85 ^{o}C, but moderately between 85 and 135 ^{o}C.
3. The peak and post-peak strength envelopes were nonlinear with a pronounced curvature at low mean stresses (close to the zone of tensile failure) and could be described well by a temperature-dependent power relationship.
4. The drained heating tests under constant isotropic stress produced volume changes that depended mainly on the stress history, i.e. the overconsolidation ratio (OCR). Heating of the sample with OCR=1.7 produced thermal contraction while all other samples, OCR=2.9 and 8.6, showed thermal expansion followed by thermal contraction (samples with higher OCRs expanded more).

According to the aforementioned characteristics the temperature-dependent behaviour of the Colorado shale is different from normal clays, in that firstly the elastic moduli are pronouncedly temperature-dependent and secondly the critical friction angle decreases at elevated temperatures. Furthermore, the evidence of structuration, i.e. observation 1 above, is recognizable even at elevated temperatures (Mohamadi and Wan 2015b). Proper description of these constitutive features entails recourse to a robust thermo-elasto-plastic constitutive models as discussed in the next subsection.

3 THERMO-ELASTOPLATIC MODELING

3.1 Preliminaries

All the stresses in this study are treated as effective, although for simplicity the prime usually associated with effective stresses in geomechanics is dropped. Component of the stress tensor $\boldsymbol{\sigma}$ and strain tensor $\boldsymbol{\varepsilon}$ are assumed positive in compression. The letter 'd' before the name of a variable denotes its increment, and the superscripts 'e', 'p', 'σ' and 'T' designate the elastic, plastic, stress-induced and temperature-induced components, respectively, e.g. $\varepsilon_v^{p\sigma}$ denotes the stress-induced plastic volumetric strain. The model formulation is presented in the triaxial stress/strain space where $p=(\sigma_1+2\sigma_3)/3$, $q=\sigma_1-\sigma_3$, $\varepsilon_v=\varepsilon_1+2\varepsilon_3$ and $\varepsilon_v=2(\varepsilon_1-\varepsilon_3)/3$ with σ_i and ε_i ($i=1,3$) being the major and minor principal components of the stress and strain tensor, respectively.

3.2 Isothermal model

The isothermal model used in this study was originally proposed in Nakai et al. (2011) and later on modified by Mohamadi and Wan (2015a) to account for the frictional destructuration mechanism. Herein, a brief review of the model is presented for the later extension to non-isothermal conditions.

The central premise of the isothermal model is the subloading surface, (Hashiguchi and Ueno 1977), defined as a surface that always passes over the current stress point and is geometrically similar to a normal yield surface. The subloading surface f in the isothermal model is a generalization of the original Cam-Clay model yield function, (Schofield and Wroth 1968), written in terms of void ratio difference ρ and frictional structuration factor R as:

$$f=\frac{1}{\beta R}\left(\frac{q}{Mp}\right)^{\beta}+\ln\frac{p}{p_0}-\frac{1}{C_p}\left(\varepsilon_v^{p}-\frac{\rho}{1+e_0}\right)=0 \qquad [1]$$

where e_0 and p_0 are the reference void ratio and mean stress, respectively, M is the slope of the critical state line of a reconstituted sample, $\beta\geq 1$ is a model parameter controlling the shape of the subloading surface and $C_p=(\lambda-\kappa)/(1+e_0)$ where λ and κ are the slopes of normal compression line and unloading-reloading line in the $e-\ln p$ plane, respectively. The plastic volumetric strain ε_v^p is a model internal variable whose increment can be linked to a positive plastic multiplier $d\Lambda$ through adoption of an associated flow rule, i.e.

$$d\varepsilon_v^p = d\Lambda \frac{\partial f}{\partial p} \quad [2]$$

Upon loading, the subloading surface expands faster than the normal yield surface until completely coinciding with it. The rate of the convergence between the subloading and the normal-yield surface is controlled by the void ratio difference ρ, i.e.

$$d\rho = -(1+e_0)(\frac{a\rho}{p} + \frac{b\omega}{p})d\Lambda \quad [3\text{-a}]$$

$$d\omega = -(1+e_0)(\frac{b\omega}{p})d\Lambda \quad [3\text{-b}]$$

where ω is an imaginary density-like internal variable representing the effect of isotropic structuration and a and b are two new material parameters controlling the pace of overconsolidation degradation and isotropic destructuration, respectively. In fact, existence of ω in Eq. [3-a] makes it possible to move the stress state towards the right of the normal consolidation line, which is deemed impossible in unstructured soils. Structuration also changes the critical friction angle of the material, a feature that is controlled by the frictional structuration factor R whose increment is given by

$$dR = -(\frac{c\ln R}{p})d\Lambda \quad [4]$$

where c is another material parameter controlling the pace of frictional destructuration. Recalling that the current stress state invariably lies on the subloading surface, one does not need to determine whether the stress state reaches the yield surface, and hence, the loading condition is given by

$$\begin{cases} d\boldsymbol{\varepsilon}^p \neq 0 & \text{if} \quad d\Lambda > 0 \\ d\boldsymbol{\varepsilon}^p = 0 & \text{otherwise} \end{cases} \quad [5]$$

Finally, the elastic behaviour is assumed to be governed by the Hook's law, i.e.

$$d\varepsilon_v^e = \frac{dp}{K} \quad \& \quad d\varepsilon_q^e = \frac{dq}{3G} \quad [6]$$

where bulk modulus K and shear modulus G are those used in the original Cam-Clay model with the assumption of constant Poisson's ratio ν , i.e. $K=(1+e_0)p/\kappa$ and $G=3(1-2\nu)K/2(1+\nu)$, and $d\varepsilon_v^e$ and $d\varepsilon_q^e$ are the incremental elastic volumetric and shear strain, respectively.

3.3 Non-Isothermal model

Different constitutive features of the isothermal model such as the elastic rule, plastic flow and subloading and normal-yield surface need to be adapted for non-isothermal conditions.

3.3.1 Thermo-elastic behaviour

As mentioned earlier, the initial stiffness of the Colorado shale determined from triaxial compression tests decreased at elevated temperatures. To implement this feature in the isothermal model, the incremental elastic volumetric strain $d\varepsilon_v^e$ was additively decomposed into mechanical $d\varepsilon_v^{e\sigma}$ and thermal $d\varepsilon_v^{eT}$ components as:

$$d\varepsilon_v^e = d\varepsilon_v^{e\sigma} + d\varepsilon_v^{eT} = \frac{\kappa(T)}{p(1+e_0)}dp + \frac{\xi(T,p)}{1+e_0}dT \quad [7]$$

where $\kappa(T)$ is the slope of isotropic unloading-reloading line in $e-\ln p$ plane at temperature T and $\xi(T,p)$ is a pressure- and temperature-dependent thermal parameter. Based on the experimental observations on the Colorado shale $\kappa(T)=\kappa_0[1+\beta_T\ln(T/T_0)]$ where κ_0 is the slope of unloading-reloading line in $e-\ln p$ plane at temperature T_0 and β_T is the coupling constant implying pressure-temperature coupling in volumetric strain. The temperature-dependence of the elastic parameter $\kappa(T)$ entails pressure-dependence of the thermal parameter $\xi(T,p)$ such that the thermo-elastic volumetric strain is path-independent, i.e. the elastic strain shall not depend on the order of application of the incremental temperature and mean stress. Herein, the form of $\xi(T,p)$ which satisfies is chosen as:

$$\xi(T,p) = \alpha_T + \frac{\kappa_0\beta_T}{T}\ln\frac{p}{p_{c0}} \quad [8]$$

where α_T is the cooling compression index and p_{c0} is the preconsolidation pressure at temperature T_0. The value of α_T can be either negative (compression due to cooling), e.g. see (Abuel-Naga et al. 2007; Sultan et al. 2002; Towhata et al. 1993), or positive (expansion due to cooling), e.g. see (Baldi et al. 1988; Campanella and Mitchell 1968; Graham et al. 2001; Hueckel and Baldi 1990). Incremental elastic shear strain $d\varepsilon_q^e$ is assumed to be purely mechanical, that is being merely induced by the incremental deviatoric stress dq as $d\varepsilon_q^e = dq/3G(T,p)$ where $G(T,p)=3(1-2\nu)(1+e_0)p/2(1+\nu)\kappa(T)$.

3.3.2 Thermo-plastic behaviour

As mentioned earlier, the isothermal model is an extension of the original Cam-clay model, and hence makes use of volumetric hardening mechanism which in non-isothermal conditions shall be modifiedto account for the shrinkage of yield limit at elevated temperatures. Invoking the parallel downward shift of the normal consolidation line, the simplest form for the reference void ratio at temperature T, i.e. e_T, is chosen, i.e.

$$e_T = e_0 - \lambda_T (T - T_0) \qquad [9]$$

where e_0 is the reference void ratio at temperature T_0 and λ_T is the heating compression index which represents the slope of the thermal consolidation line at constant isotropic stress in $e-T$ plane. Making use of Eq. [7] in conjunction with the additive decomposition of the volumetric strain into elastic and plastic parts, Eq. [9] can be used to obtain the incremental plastic volumetric strain $d\varepsilon_v^p$ as:

$$d\varepsilon_v^p = \frac{\lambda - \kappa(T)}{(1+e_0)p} dp + \frac{\lambda_T - \xi(T,p)}{1+e_0} dT \qquad [10]$$

Considering that Eq. [10] is path-independent, the preconsolidation pressure at temperature T can be formulated as:

$$p_{cT} = p_0 \exp\left[\frac{\begin{pmatrix} (1+e_0)\varepsilon_v^p - (\lambda_T - \alpha_T)(T - T_0) \\ +\kappa_0 \beta_T \ln \frac{T}{T_0} \ln \frac{p_0}{p_{c0}} \end{pmatrix}}{\lambda - \kappa(T)}\right] \qquad [11]$$

Eq. [11] is quite useful in generalizing the normal-yield and subloading surface to non-isothermal conditions as discussed in the next subsection.

Another plastic mechanism that needs to be modified at elevated temperatures, is the incremental dissipated energy dw^p which in the isothermal model is given by $dw^p = pd\varepsilon_v^p + qd\varepsilon_q^p = Rq(Mp/q)^\beta d\varepsilon_q^p$. It is observed that dissipated energy depends on both β and M. The former controls the shape of the yield surface and is assumed to be constant herein while the latter is assumed to follow a linear relationship at elevated temperatures, i.e.

$$M_T = M_0 - \gamma_T (T - T_0) \qquad [12]$$

where M_0 and M_T are slopes of the critical state lines at temperatures T_0 and T, respectively, and γ_T is a positive material constant to capture thermal reduction of the critical strength as mentioned earlier in the case of the Colorado shale.

3.3.3 Non-isothermal subloading and normal-yield surface

Similar to Eq. [1], the normal-yield surface at elevated temperatures writes:

$$F = \frac{1}{\beta R}\left(\frac{\bar{q}}{M_T \bar{p}}\right)^\beta + \ln\left(\frac{\bar{p}}{p_{cT}}\right) = 0 \qquad [13]$$

where $(\bar{p}, \bar{q})$ is a point on the normal-yield surface at a given temperature T. Combining Eq. [11] and [13], the subloading surface at temperature T writes

$$f = \frac{1}{\beta R}\left(\frac{q}{M_T p}\right)^\beta + \ln\left(\frac{p}{p_0}\right) - \frac{1}{\lambda - \kappa(T)} \left((1+e_0)\varepsilon_v^p - (\lambda_T - \alpha_T)(T - T_0) + \kappa_0 \beta_T \ln\frac{T}{T_0}\ln\frac{p_0}{p_{c0}} - \rho\right) = 0 \qquad [14]$$

The three-dimensional view of the normal-yield and subloading surface in $q-p-T$ space at a constant plastic volumetric strain is presented in Fig. 1.

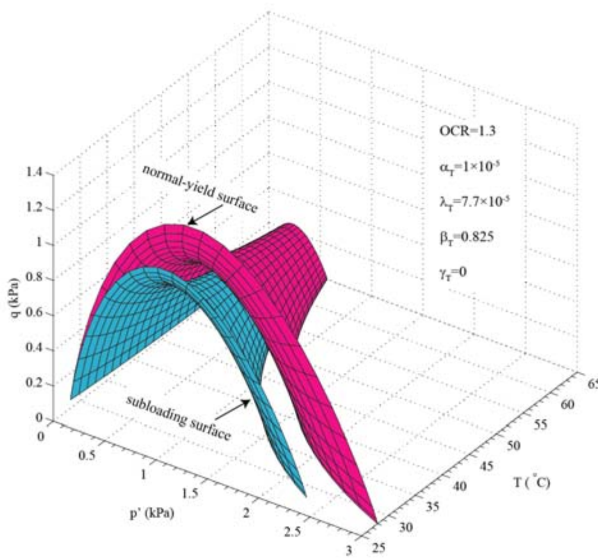

Figure 1. 3-Dimensional view of the non-isothermal subloading and normal-yield surface at constant plastic volumetric strain.

3.3.4 Thermo-Elastoplastic constitutive equation

Applying consistency condition ($df = 0$) to Eq. [14], the positive plastic multiplier $d\Lambda$ can be formulated as:

$$d\Lambda = \frac{f_{,p}dp + f_{,q}dq + f_{,T}^* dT}{\frac{(1+e_0)}{\lambda - \kappa(T)}\left(f_{,p} + \frac{a\rho}{p} + \frac{b\omega}{p}\right) + f_{,R}\frac{c\ln R}{p}}$$

$$f_{,T}^* = f_{,M_T} M_{T,T} + \frac{\lambda_T - \xi(T,p) - \frac{\kappa_0 \beta_T}{\beta R T}\left(\frac{q}{M_T p}\right)^\beta}{\lambda - \kappa(T)} \qquad [15]$$

where $y_{,x}$ denotes the partial derivative of y with respect to x. The loading criterion in non-isothermal conditions is given by Eq. [5] with $d\Lambda$ given in Eq. [15]. Recalling the additive decomposition of the total incremental strain into elastic and plastic components, the thermo-elastoplastic constitutive equation in a stress-temperature-controlled program can be readily formulated as:

$$\begin{Bmatrix} d\varepsilon_v \\ d\varepsilon_q \end{Bmatrix} = \begin{bmatrix} \frac{\kappa(T)}{1+e_0} + \frac{f_{,p}^2}{H_{pT}} & \frac{f_{,p} f_{,q}}{H_{pT}} & \frac{\xi(T,p)}{1+e_0} + \frac{f_{,p} f_{,T}^*}{H_{pT}} \\ \frac{f_{,p} f_{,q}}{H_{pT}} & \frac{1}{3G(T,p)} + \frac{f_{,q}^2}{H_{pT}} & \frac{f_{,q} f_{,T}^*}{H_{pT}} \end{bmatrix} \begin{Bmatrix} dp \\ dq \\ dT \end{Bmatrix} \quad [16]$$

$$H_{pT} = \frac{(1+e_0)}{\lambda - \kappa(T)} \left(f_{,p} + \frac{a\rho}{p} + \frac{b\omega}{p} \right) + f_{,R} \frac{c \ln R}{p}$$

It is noteworthy that by setting $\beta_T = \gamma_T = 0$ and doing simple manipulations, Eq. [16] would reduce to those reported in Nakai et al (2011).

4 MODEL ASSESSMENT

Model simulations as per Eq. [16] were employed to reproduce results of drained heating and drained isothermal triaxial compression tests at different temperatures, on Colorado shale. The elaborate discussions of the corresponding experimental results were presented in Mohamadi and Wan (2015b) to which the interested reader is referred.

The first step in the proper simulation of the material behaviour using the proposed model is determination of the material parameters. The isothermal model requires evaluation of two elastic parameters, i.e. κ_0, ν, four elastoplastic parameters, i.e. e_0, λ, M, β, and three evolution parameters, i.e. a, b, c. In view of the proposed thermo-elastoplastic mechanisms four new material parameters, i.e. $\alpha_T, \beta_T, \gamma_T, \lambda_T$, are added to the model. As discussed by Nakai et al.(2011) and Mohamadi and Wan (2015a), all parameters in the isothermal model can be determined form well-established geotechnical experiments and will not be further explained here. However, particular attention will be given to the calibration procedure for the thermal parameters $\alpha_T, \beta_T, \gamma_T, \lambda_T$ in the case of the Colorado shale.

As mentioned earlier the post-peak strength, i.e. the critical state strength, of the Colorado shale varies with confining stress. Considering the uniqueness of the critical state envelope in the stress space, one can readily associate initial confining pressure (given the stress path) with the slope of a secant critical state line $M_{\sec}$ connecting origin of the stress space to the current critical point. In the case of the Colorado shale, $M_{\sec}$ at different temperatures can be described with parallel logarithmic relationships whose intercepts with the line $p_0 = 1\,MPa$ decrease linearly with augmentation of temperature, i.e. $M_{\sec}^T = M_{\sec}^{T_0} - \gamma_T (T - T_0)$ where $M_{\sec}^T$ is the secant critical slope at temperature T, $M_{\sec}^{T_0} = 1.3462 - 0.3743 \ln p_0$ is the secant critical slope at temperature T_0 and $\gamma_T = 0.0048$.

This parameter β_T is responsible for variations of the elastic moduli with temperature. The best experiment for calibration of the parameter β_T is the isothermal isotropic unloading-reloading test performed at different temperatures. However, in the case of practical applications for which results of such experiments are mostly unavailable, one can calibrate β_T using the values of Young's moduli determined from isothermal drained triaxial compression tests at different temperatures. Based on the earlier discussions in sub-section 3.3.1, the ratio between Young's modulus at elevated temperatures E and that at ambient temperature E_0 is given by $E / E_0 = (1 + \beta_T \ln(T / T_0))^{-1}$. This equation is plotted along with the experimental data points of the Colorado shale in Fig. 2 where $\beta_T = 0.9035$.

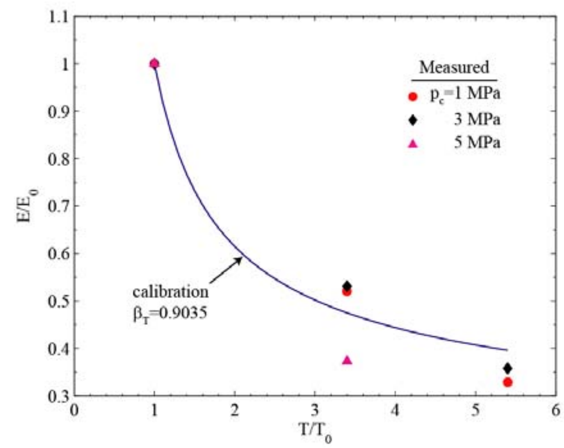

Figure 2. Calibration of the thermoelastic coupling term β_T based on the Young's moduli.

Having determined β_T, the thermal compression indices, i.e. λ_T, α_T, can be calibrated based on the results of the drained heating and cooling tests on isotropically loaded samples. Fig. 3 shows the plot of thermal volumetric strain of the Colorado shale samples with different OCRs. It is observed that the volumetric strains are affected by the stress history of the samples, that is the higher the initial OCR the larger the expansive volume changes. Due to lack of cooling tests on the samples, the cooling compression index $\alpha_T = 4.7 \times 10^{-5}$ was calibrated based on the test results at the intermediate OCR, i.e. 2.88, which was also employed to calibrate the value of heating compression index $\lambda_T = 3 \times 10^{-4}$. Table 2 reports other model parameters in the case of the Colorado shale together with the initial values of the internal parameters.

Using the determined material parameters, the volume changes of the samples at OCR=8.65 and 1.73 were predicted as shown in Fig. 3. It is observed that model predictions agree with test data of OCR=8.65 reasonably well but under-predict that at OCR=1.73. The latter can be attributed to variability of the natural samples as well as the simplifying assumption of employing one yield surface to describe both pressure- and temperature-induced volume changes. A better prediction of the thermal volume changes can be obtained if the yield limit in the

$p-T$ plane is assumed to be composed of two coupled parts, namely, the loading yield (LY) and the thermal yield (TY), as described by Cui et al. (2000). However, this approach introduces too many material parameters in the model, and hence brings about complexity in the modeling.

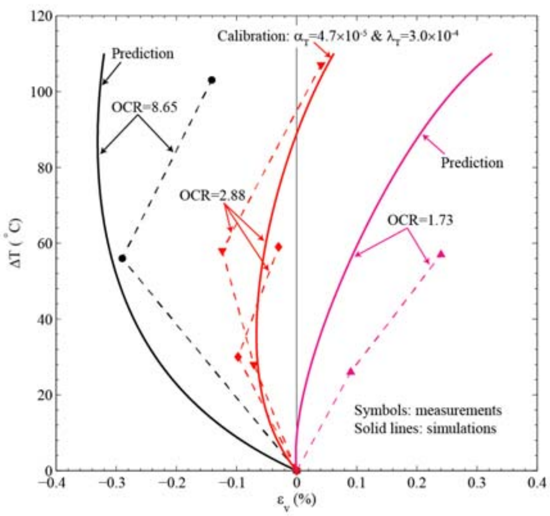

Figure 3. Behaviour of Colorado shale due to heating under constant isotropic stress together with model simulations.

Table 1. Model parameters for the Colorado shale.

Parameter	value
e_0	0.5586 @ 0.1 kPa
λ	0.0201
κ_0	0.0034
ν	0.34
β	3.5
a	900
b	50
c	400
ρ_0	$(\lambda-\kappa_0)\ln OCR$
ω_0	0.5
R_0	1.0

5 SUMMARY AND CONCLUSIONS

The constitutive study of the non-isothermal behaviour of geomaterials in the context of continuum theory of plasticity is usually performed as perobserved phenomenological mechanisms. Based on the experimental observations on the Colorado shale, the temperature-dependency of the elastic moduli and the thermal variability of the critical state line in the stress space were implemented in the constitutive model of Nakai et al.(2011). A coupled thermodynamically admissible thermoelastic rule was proposed and employed to formulate the generic form for the family of the loading yield curves. In view of the latter, the subloading and normal-yield surfaces were extended to non-isothermal conditions. The new model was applied to successfully simulate the behaviour of the Colorado shale. For the ongoing research, it is desired to incorporate the effects of temperature variations on destructuration mechanisms in the proposed model.

ACKNOWLEDGEMENTS

The authors would like to thank the Natural Sciences and Engineering Research Council of Canada (NSERC) and the CMG Foundation for providing financial support of this research through a CRD grant.

REFERENCES

Abuel-Naga, H.M., Bergado, D.T., Bouazza, A., and Ramana, G.V. 2007. Volume change behaviour of saturated clays under drained heating conditions: experimental results and constitutive modeling. Canadian Geotechnical Journal 44(8): 942-956. doi: 10.1139/t07-031.

Abuel-Naga, H.M., Pender, M., Bergado, D.T., and Bouazza, A. 2009. Thermomechanical model for saturated clays. geotechnique 59(3): 273-278.

Baldi, G., Hueckel, T., and Pellegrini, R. 1988. Thermal Volume Changes of the Mineral Water-System in Low-Porosity Clay Soils. Canadian Geotechnical Journal 25(4): 807-825. doi: Doi 10.1139/T88-089.

Burland, J.B. 1990. On the compressibility and shear strength of natural clays. Geotechnique 40(3): 329-378.

Campanella, R.G., and Mitchell, J.K. 1968. Influence of temperature variations in soil behaviour. Journal of the Soil Mechanics and Foundations Division 94(3): 709-734.

Carlson, M. 2012. An Analysis of the Caprock Failure at Joslyn. SPE-156962.

Cekerevac, C., and Laloui, L. 2004. Experimental study of thermal effects on the mechanical behaviour of a clay. International Journal for Numerical and Analytical Methods in Geomechanics 28(3): 209-228. doi: Doi 10.1002/Nag.332.

Collins, P.M. 2007. Geomechanical effects on the SAGD process. Spe Reserv Eval Eng 10(4): 367-375.

Cui, Y.J., Sultan, N., and Delage, P. 2000. A thermomechanical model for saturated clays. Canadian Geotechnical Journal 37: 607-620.

Graham, J., Tanaka, N., Crilly, T., and Alfaro, M. 2001. Modified Cam-Clay modelling of temperature effects in clays. Canadian Geotechnical Journal 38(3): 608-621. doi: 10.1139/t00-125.

Hamidi, A., Tourchi, S., and Khazaei, C. 2015. Thermomechanical Constitutive Model for Saturated Clays Based on Critical State Theory. International Journal of Geomechanics 15(1): 04014038. doi: doi:10.1061/(ASCE)GM.1943-5622.0000402.

Hashiguchi, K., and Ueno, M. 1977. Elastoplastic constitutive laws of granular materials. *In* Constitutive equations of soils. *Edited by* S. Murayama and A.N. Schofield. JSSMFE, Tokyo. pp. 73-82.

Hueckel, T., and Baldi, G. 1990. Thermoplasticity of Saturated Clays: Experimental Constitutive Study. Journal of Geotechnical Engineering 116(12): 1778-1796. doi: doi:10.1061/(ASCE)0733-9410(1990)116:12(1778).

Hueckel, T., and Borsetto, M. 1990. Thermoplasticity of Saturated Soils and Shales: Constitutive Equations. Journal of Geotechnical Engineering 116(12): 1765-1777. doi: doi:10.1061/(ASCE)0733-9410(1990)116:12(1765).

Laloui, L., and Cekerevac, C. 2003. Thermo-plasticity of clays: An isotropic yield mechanism. Computers and Geotechnics 30(8): 649-660. doi: http://dx.doi.org/10.1016/j.compgeo.2003.09.001.

Leroueil, S., and Vaughan, P.R. 1990. The general and congruent effects of structure in natural soils and weak rocks. Geotechnique 45(3): 467-488.

Liu, E.L., and Xing, H.L. 2009. A double hardening thermo-mechanical constitutive model for overconsolidated clays. Acta Geotech. 4(1): 1-6. doi: 10.1007/s11440-008-0053-4.

Mohamadi, M., and Wan, R.G. 2015a. Influence of Structuration on the Critical State Friction Angle: an Elastoplastic Description. *In* The 49th US Rock Mechanics/Geomechanics Symposium, California. pp. ARMA 15-668.

Mohamadi, M., and Wan, R.G. 2015b. Strength and post-peak response of Colorado shale at high pressure and temperature. under review.

Monfared, M., Sulem, J., Delage, P., and Mohajerani, M. 2011. A Laboratory Investigation on Thermal Properties of the Opalinus Claystone. Rock Mech Rock Eng 44(6): 735-747. doi: 10.1007/s00603-011-0171-4.

Nakai, T., Shahin, H.M., Kikumoto, M., Kyokawa, H., Zhang, F., and Farias, M.M. 2011. A Simple and Unified Three-Dimensional Model to Describe Various Characteristics of Soils. Soils and Foundations 51(6): 1149-1168.

Robinet, J.C., Rahbaoui, A., Plas, F., and Lebon, P. 1996. A constitutive thermomechanical model for saturated clays. Engineering Geology 41(1–4): 145-169. doi: http://dx.doi.org/10.1016/0013-7952(95)00049-6.

Schofield, A.N., and Wroth, C.P. 1968. Critical State Soil Mechanics. McGraw-Hill. pp. 310.

Sultan, N., Delage, P., and Cui, Y.J. 2002. Temperature effects on the volume change behaviour of Boom clay. Engineering Geology 64: 135-145.

Tanaka, N., Graham, J., and Crilly, T. 1997. Stress-strain behaviour of reconstituted illitic clay at different temperatures. Engineering Geology 47(4): 339-350. doi: http://dx.doi.org/10.1016/S0013-7952(96)00113-5.

Towhata, I., Kuntiwattanaku, P., Seko, I., and Ohishi, K. 1993. Volume Change of Clays Induced by Heating as Observed in Consolidation Tests. Soils and Foundations 33(4): 170-183.

Yao, Y.P., and Zhou, A.N. 2013. Non-isothermal unified hardening model: a thermo-elasto-plastic model for clays. geotechnique 63(15): 1328-1345.

Zhang, S., Leng, W., Zhang, F., and Xiong, Y. 2012. A simple thermo-elastoplastic model for geomaterials. International Journal of Plasticity 34(0): 93-113. doi: http://dx.doi.org/10.1016/j.ijplas.2012.01.011.

Zhou, C., and Ng, C.W.W. 2015. A thermomechanical model for saturated soil at small and large strains. Canadian Geotechnical Journal: 1-10. doi: 10.1139/cgj-2014-0229.